J Solid State Electrochem (2009) 13:1339–1350
DOI 10.1007/s10008-008-0679-z

ORIGINAL PAPER

Study of the optimal condition for electroplating of Bi_2S_3 thin films and their photoelectrochemical characteristics

Atanu Jana · Chinmoy Bhattacharya · Subrata Sinha · Jayati Datta

Received: 29 March 2008 / Revised: 5 September 2008 / Accepted: 9 September 2008 / Published online: 8 October 2008

Abstract Bismuth sulfide (Bi_2S_3) thin films were electrodeposited from non-aqueous dimethyl sulfoxide medium containing $Bi(NO_3)_3$ and thiourea as the precursor salts, triethanol amine as the complexing agent, and TritonX-100 as the surface active agent. The prepared films were subjected to rigorous experimentation in order to validate their potential candidature for solar cells. The films exhibited band gap energy of ~1.3 eV and resistivity of the order of 2×10^6 Ω cm at room temperature as was obtained from UV–Vis spectroscopy and four-probe measurements, respectively. Scanning electron microscopy, transmission electron microscopy, X-ray diffraction, and energy dispersive analysis of X-ray were employed to reveal the morphology, structure, and chemical composition of the film matrix. The Bi_2S_3 films were found to be non-decomposable up to the temperature of 1,000 °C with the help of thermogravimetry–differential thermal analysis. The Nyquist and Mott–Schottky plots derived from electrochemical impedance spectroscopy measurements provided important information regarding electrical and semiconducting properties of the films. The *n*-type film with a donor density of the order of $\sim10^{23}$ m^{-3} displayed reasonable photoactivity under illumination and is recommended as a promising candidate for potential photoelectrochemical applications.

A. Jana · C. Bhattacharya · J. Datta (✉)
Department of Chemistry,
Bengal Engineering and Science University,
Shibpur,
Howrah 711 103 West Bengal, India
e-mail: jayati_datta@rediffmail.com

S. Sinha
Department of Chemistry, Mahadebananda Mahavidyalaya,
Monirampur, Barrackpore,
24 Parganas (N), India

Keywords Nanocrystalline Bi_2S_3 thin films · Electrochemical deposition · TG–DTA · Photoelectrochemical cell · Electrochemical impedance spectroscopy

Introduction

During the last few years, there is an upsurge of interest in developing thin films of different semiconductor (SC) materials for their applications in solar selective coating, solar cells, sensors, optical mass memories, γ-ray detection and so on [1–7]. Among the different Gr.V metal chalcogenides (M^VX^{VI}), bismuth sulfide (Bi_2S_3) poses to be one of the attractive materials for photoanode in photoelectrochemical (PEC) solar cells. This is due to its forbidden energy gap lying between 1.25 and 1.70 eV, near to the range of theoretically maximum attainable energy conversion efficiency [8–12]. Further quantum size effect of non-crystalline Bi_2S_3 films shows the significant changes in PEC cell performance [13, 14].

Various methods such as chemical bath deposition from aqueous or non-aqueous medium, spray, vacuum evaporation, sol-gel, and electrochemical deposition have been used for developing Bi_2S_3 film [14–21]. The application criteria of these materials depend on the chemical composition and crystalline structure of the film matrix. In the present study, we have successfully developed Bi_2S_3 films from non-aqueous dimethyl sulfoxide (DMSO) bath on conducting substrates through electrodeposition technique, one of the simple and cost-effective methods of preparing thin films. During deposition, the controlling parameters like bath concentrations, deposition current density, and temperature were optimized to obtain the best performing semiconductor film.

Surface morphology, structure, and composition of the film matrix were studied through scanning electron microscopy (SEM), transmission electron microscopy (TEM), X-ray diffraction (XRD), and energy dispersive analysis of X-ray (EDAX) techniques, respectively, and the stability of the film was ensured by thermogravimetry–differential thermal analysis (TG–DTA). Electrochemical impedance spectroscopy and current–potential measurements were recorded to characterize the electrochemical behavior of the semiconductor–electrolyte interface in dark and illuminated conditions.

Experimental

Deposition of Bi_2S_3 thin film

Electrodeposition of bismuth trisulfide thin films has been carried out under galvanostatic mode on transparent conducting oxide [TCO, F-doped SnO_2]-coated glass substrates [BHEL, India] in non-aqueous DMSO bath containing respective precursor salts, cationic—$Bi(NO_3)_3$ and anionic—thiourea, with a variable amount of triethanol amine (TEA) as the complexing agent and TX-100 as the neutral surfactant. The respective deposition conditions were maintained by keeping the bath temperature within the range of 80–120 °C, current density 1–6 A m^{-2}, concentration of TEA 0.1–0.5 M and the amount of TX-100 0.1–1.0%. The neutral surfactant adds to the cohesiveness of the film onto the glass substrate [1]. After deposition, the films were washed with double distilled water and air-dried (Scheme 1).

Optical characterizations and thickness measurement

The transmittance spectrum covered the range 350 to 1100 nm for each of the as-deposited Bi_2S_3 film during measurement in JASCO V-530 UV–VIS–NIR Spectrophotometer, Japan, and band gap was calculated from the differential transmittance plot. The thickness of the deposited thin films was determined gravimetrically using the relation,

$$t = m/\rho A \quad (1)$$

where, m and A stand for mass and area of the deposited film, and ρ the density of the film was taken to be 6,780 kg m^{-3}.

Surface characterizations by SEM–EDAX, TEM, and XRD analysis

The prepared films were subjected to scanning electron microscopy in a JEOL JSM-6700F FESEM to observe the morphology of the surface. The compositions of the films were subsequently determined by energy dispersive analysis of X-ray. Philips PW 1710, X-ray diffractometer was employed using CuKα radiation with wavelength 1.542 Å, to study the crystallinity of the surface. The X-ray machine was operated on 25 kV, 20 mA within the 2θ range of angles between 20° and 60° and 2θ increment of 0.02°. Powdered samples of the film materials were subjected to transmission electron microscopy using PHILIPS CM 12 HRTEM with an accelerating voltage of 200 kV.

Thermal gravimetry and differential thermal analysis

The thermal properties of Bi_2S_3 thin films were determined using the TG–DTA technique using N535-0010 diamond TG/DTA analyzer, Perkin Elmer, USA. The film materials were subjected to controlled temperature within the range of 50–1,000 °C, and the mass of the sample under consideration was measured as a function of temperature. The heating rate employed was 20 °C min^{-1} in nitrogen atmosphere.

Electrochemical characterizations through EIS technique

The electrochemical impedance spectroscopic (EIS) measurements were carried out at room temperature with the help of AUTOLAB 12 PG- stat, Eco-Chemie BV (The Netherlands) combined with a frequency response analyzer using a standard three-electrode cell having configuration (TCO) $Bi_2S_3/S^{2-} - S_x^{2-}$, 0.5 M/Pt, assembled with a reference-saturated calomel electrode. The impedance spectra at the respective open circuit potentials (OCP) in 0.5 M Na_2S_x electrolyte were recorded applying sinusoidal perturbation of 5 mV amplitude at the working electrode (SC) over a frequency range of 0.1 to 10 MHz. The corresponding Nyquist plots were analyzed to evaluate the equivalent circuit (EC) parameters [1, 22]. Capacitance measurements of the semiconductor electrode in contact with 0.5 M aqueous $S^{2-} - S_x^{2-}$ electrolyte were performed using the same experimental set up with an oscillator frequency of 1 kHz. The semiconductor characteristics and donor densities were determined from the Mott–Schottky plots.

Transient photoresponse

The photoresponse of each of the films was recorded in terms of rise and decay of short circuit current (I_{sc}) with a similar cell setup as employed during EIS measurement under illumination of 500 W m^{-2} using a tungsten filament light source. The decay constant was evaluated from the plot of transient photoresponse, I_{sc}−time (t) at 20 s intervals in dark and illuminated conditions.

Electrochemical characterizations of the PEC cell system

Potentiostatic polarization studies were conducted with the typical cell configuration within the potential range of −0.5 to 0.5 V employing a step potential of 0.10 V under dark and illumination of 500 W m^{-2}. Similarly, chronoamperometric measurements were performed at the respective OCP for a time span of 300 s, maintaining a constant time interval of 0.5 s. Performance of the SC films was derived in terms of photoconversion efficiency with the help of current–voltage (*I–V*) measurements under the same light intensity.

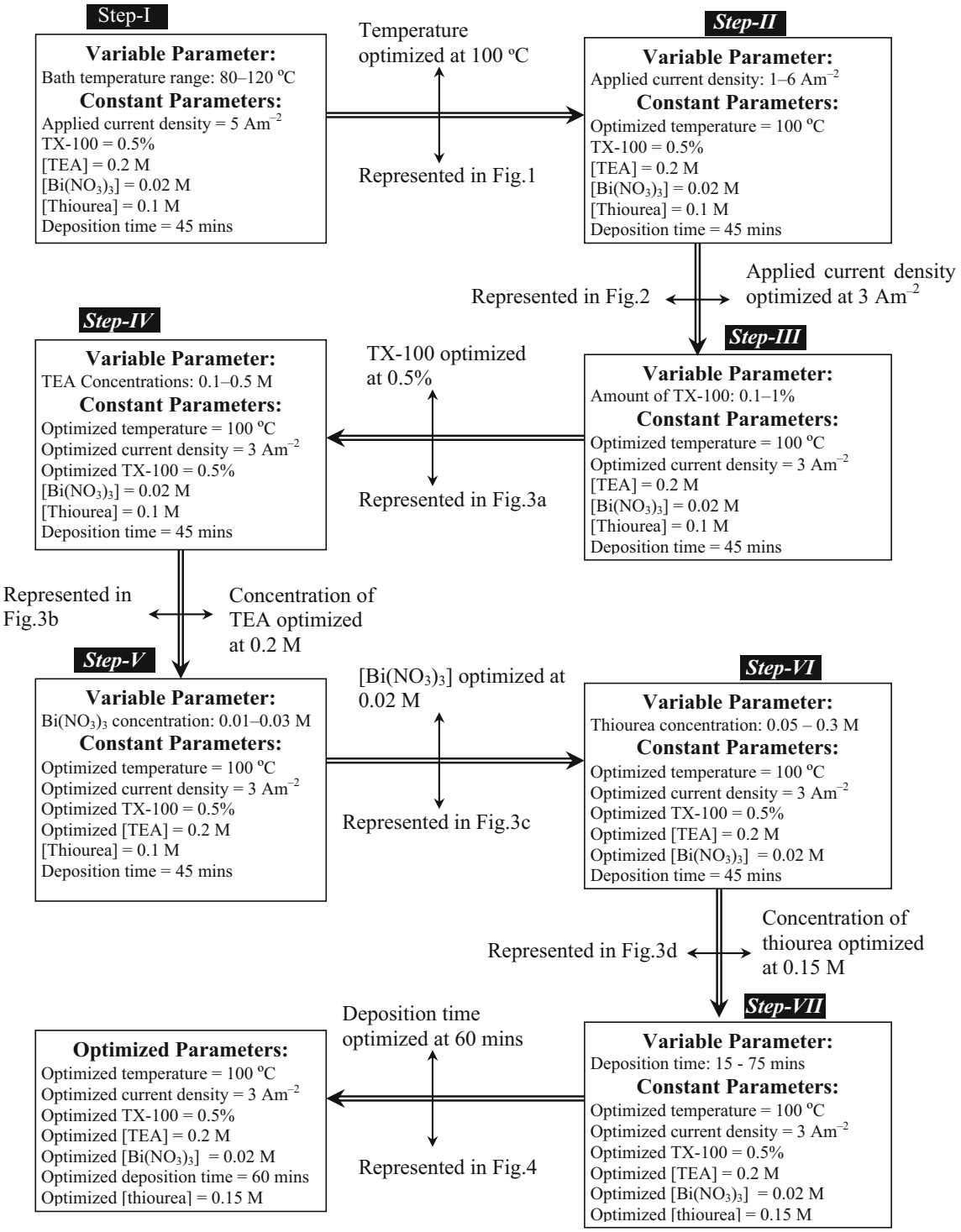

Scheme 1 Schematic representation of Bi_2S_3 film preparation through electrochemical route

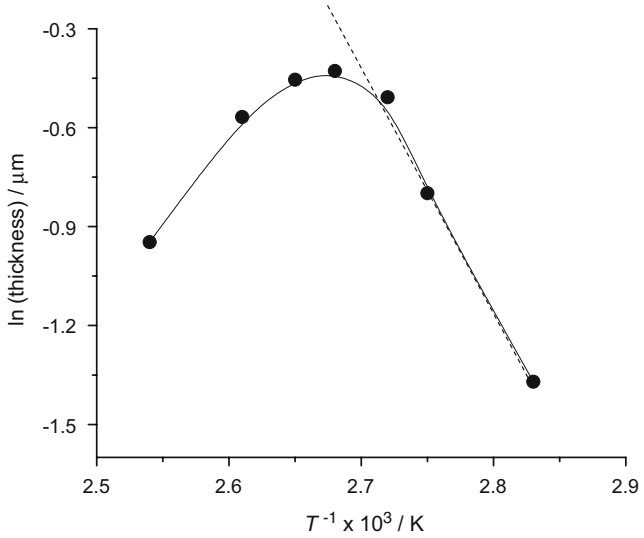

Fig. 1 Variation of film thickness (ln t/μm) with temperature (T^{-1}/K) of the electrolytic bath containing 0.02 M bismuth nitrate, 0.1 M thiourea, 0.2 M TEA, and 0.5% TX-100, and the current density and deposition time maintained at 5 A m^{-2} and 45 min, respectively

Results and discussion

During cathodic electrodeposition, the metal chalcogenide was formed on the surface of the substrate by rapid reaction of freshly adsorbed Bi^{3+}, released from the complex ion $[Bi(TEA)]^{3+}$, with the anionic precursor S^{2-} generated from dissociation of thiourea under the experimental condition. Films of various thickness were produced by successively altering the various preparative bath parameters such as deposition temperature (°C), time of deposition, applied current density (A m^{-2}), and concentration of cationic precursor (Bi^{+3}), complexing agent (TEA), and surfactant (TX-100). The band gap energies of the prepared films were found to lie within the range 1.3–1.9 eV.

At the initial stage of investigation, bath temperature was optimized within the range of 80–120 °C without changing the other parameters such as current density, concentration of Bi^{3+} and composition of the complexing agent, TX-100, and deposition time. It is observed from Fig. 1 that the film grows thicker with rise in temperature. Maximum film thickness is attained at 100 °C, beyond which the thickness gradually decreases. This behavior is presumably the reflection of the film deposition kinetics. Thickening of the film is attributed to rapid growth by faster release of Bi^{+3} and S^{2-} ions at elevated temperatures. However, when the temperature exceeds 100 °C, the film thickness diminishes as the Bi–S compound precipitates down in the bath before being deposited onto the substrate. A film with moderate thickness of ~0.6 μm is grown up with a matrix containing microcrystallites of desired size and space charge properties, as discussed later. A film with such a thickness is therefore considered the index for optimizing different parameters controlling the deposition. The thickness (ln t/μm)–temperature (T^{-1}/K) profile demonstrates pseudo-Arrhenius behavior consisting of two temperature regions, high and low, as shown in Fig. 1 [2]. The activation energy (E_{act}) of the deposition reaction was evaluated to be 56.54 kJ mol^{-1}.

The current density of 3 A m^{-2} was selected to obtain the maximum thickness of the film as shown in Fig. 2. Better adherence property of the film was achieved with TX-100 as one of the components in the deposition bath and 0.5% TX-100 appeared to be the optimum surfactant concentration. Further addition of surfactant leads to the formation of porous matrix of the film, thus reducing the compactness of the film as shown in Fig. 3a.

An optimum concentration of the complexing agent TEA was also found to be very effective in growing stable and uniform film on TCO glass substrate. TEA forms the complex $Bi[TEA]^{3+}$ with precursor $Bi(NO_3)_3$ salt and controls the reduction process by eliminating the possibility of precipitate formation in the bath [23]. Figure 3b shows that a steady growth of the film is obtained with TEA within the range of 0.15–0.25% in the deposition bath. Further addition of TEA leads to poor growth of the film as Bi^{3+} remains complexed with TEA.

In the course of varying Bi^{3+} concentration, maximum film thickness was obtained with 0.02 M $Bi(NO_3)_3$ solution as shown in Fig. 3c. Similarly, thiourea was optimized at a concentration of 0.15 M as shown in Fig. 3d. Variation of film thickness with time of deposition has been presented in Fig. 4. Film thickness was found to increase gradually with deposition time up to 60 min, beyond which the films became highly porous in nature and large cracks were clearly

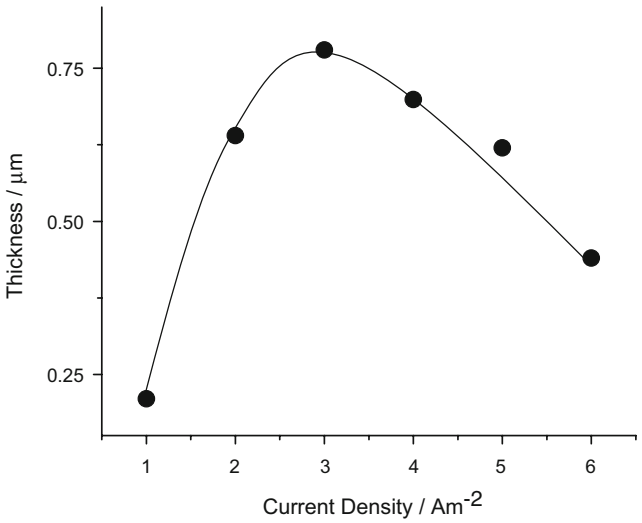

Fig. 2 Variation of film thickness (μm) with applied current density (A m^{-2}) for the electrolytic bath containing 0.02 M bismuth nitrate, 0.1 M thiourea, 0.2 M TEA, and 0.5% TX-100, and the temperature and deposition time maintained at 100 °C and 45 min, respectively

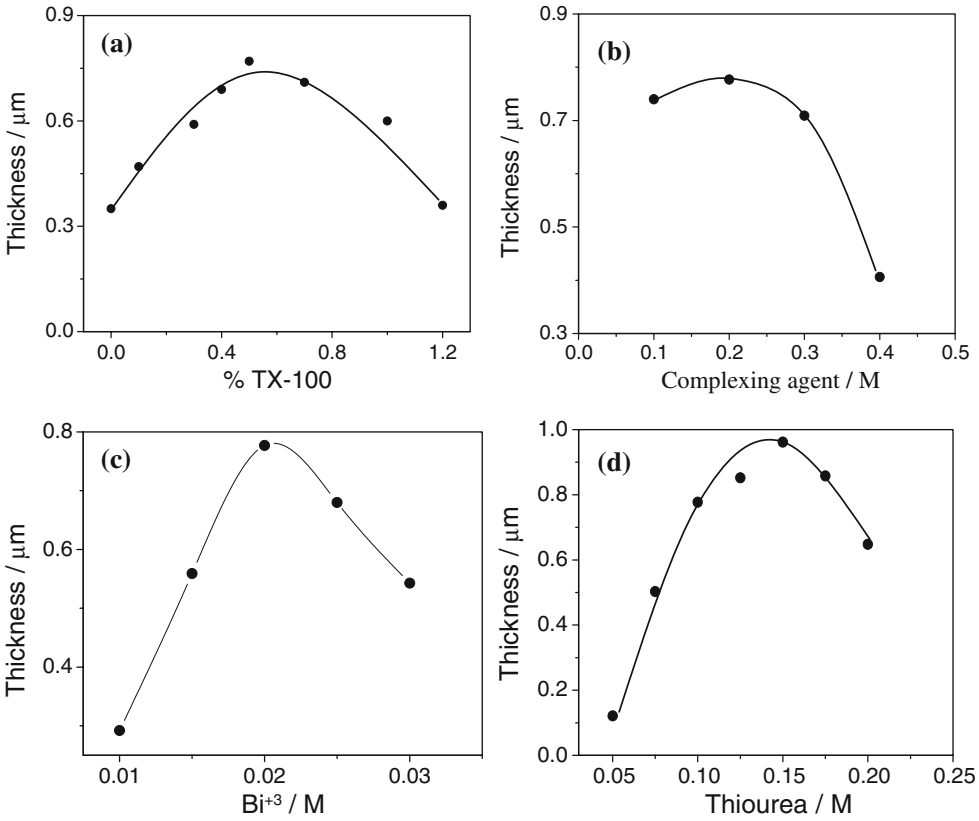

Fig. 3 **a**–**d** Variation of film thickness (µm) with **a** %TX-100, **b** concentration of TEA, **c** concentration of bismuth nitrate, and **d** concentration of thiourea in the electrolytic bath and the temperature, current density, and deposition time maintained at 100 °C, 3 A m^{-2}, and 45 min, respectively

visible on the surface. Deposition for a duration of >75 min produced film with poor adherence property.

Figure 5 shows the typical transmittance (%*T*) and differential transmittance (d*T*/dλ) spectrum of the film grown on TCO-coated glass substrate under 60 min of deposition. The sharp adsorptions edge around 950 and 710 nm, correspond to band gap energies in the region 1.3 and 1.8 eV, respectively, and are indicative of Bi_2O_3 formation along with Bi_2S_3 in the semiconductor matrix.

Typical SEM images of the material prepared under different deposition times (30, 45, and 60 min) have been presented in Fig. 6a–c. The film is found to preserve a

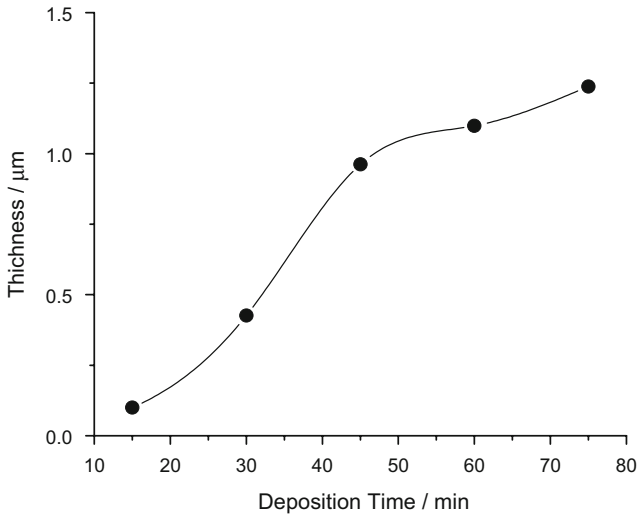

Fig. 4 Variation of film thickness (µm) with deposition time (min), for the electrolytic bath containing 0.02 M bismuth nitrate, 0.15 M thiourea, 0.2 M TEA, and 0.5% TX-100, and the temperature and current density maintained at 100 °C and 3 A m^{-2}, respectively

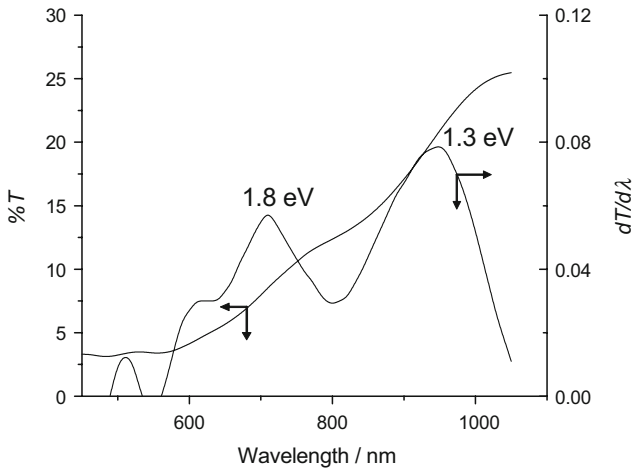

Fig. 5 Transmittance and differential transmittance spectrum of Bi_2S_3 thin film developed from the electrolytic bath containing 0.02 M bismuth nitrate, 0.15 M thiourea, 0.2 M TEA, and 0.5% TX-100 keeping current density, temperature, and deposition time at 3 A m^{-2}, 100 °C, and 60 min, respectively

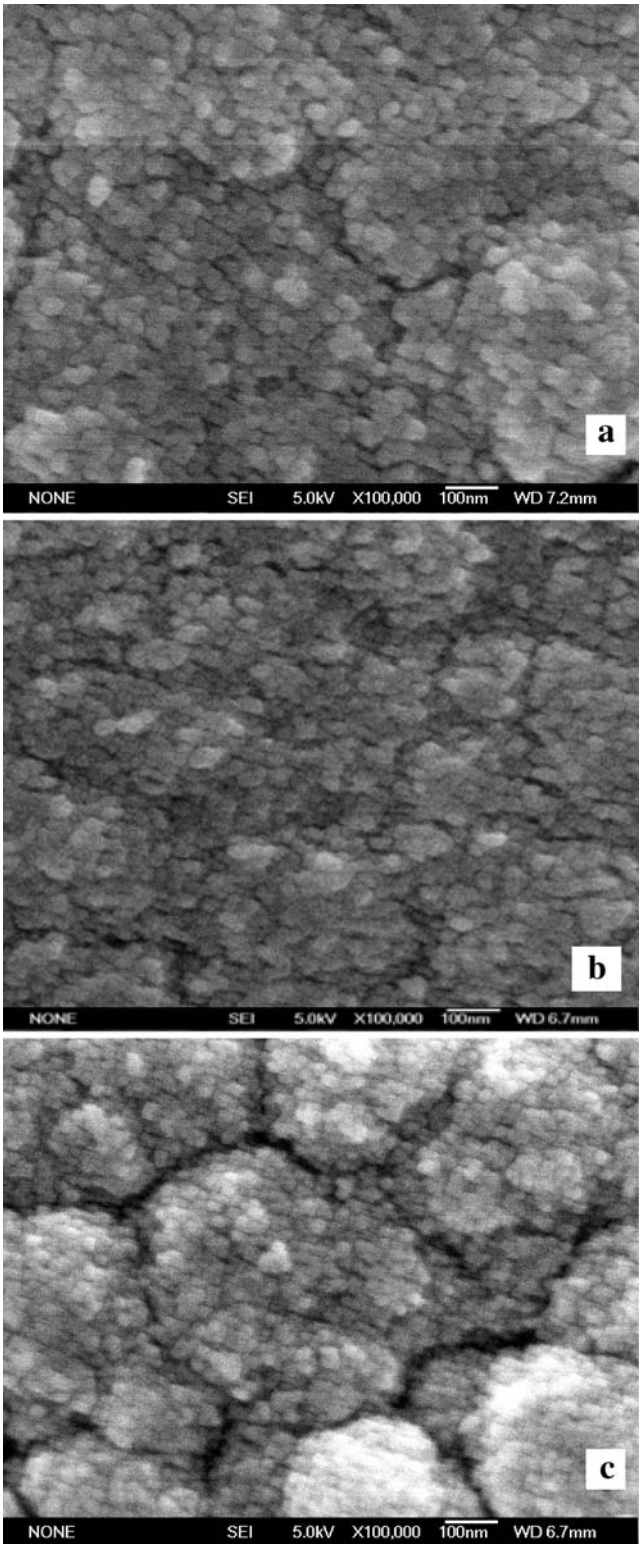

Fig. 6 **a**–**c** SEM images of Bi_2S_3 film obtained at **a** 30, **b** 45, and **c** 60 min deposition from the electrolytic bath containing 0.02 M bismuth nitrate, 0.15 M thiourea, 0.2 M TEA, and 0.5% TX-100, and the current density and temperature maintained at 3 A m^{-2} and 100 °C, respectively

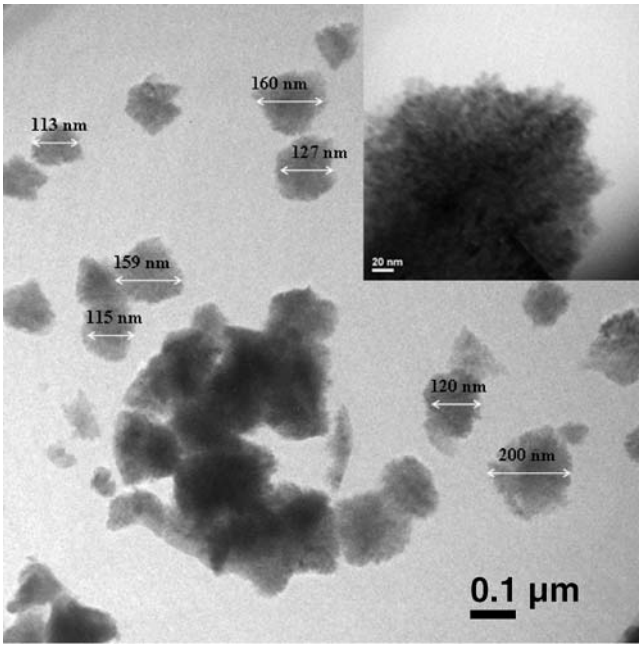

Fig. 7 TEM image of Bi_2S_3 film obtained at 60 min deposition from the electrolytic bath containing 0.02 M bismuth nitrate, 0.15 M thiourea, 0.2 M TEA, and 0.5% TX-100, and the current density and temperature maintained at 3 A m^{-2} and 100 °C, respectively

homogeneous and compact microcrystalline structure and is composed of spherically shaped well-defined grains of 15–30 nm size. The surface morphology of the prepared Bi_2S_3 films was further studied through TEM analysis. Figure 7 represents a typical TEM image of the semiconductor film prepared at 60 min deposition time and displays the compact nature of the deposits throughout the surface. The energy dispersive X-rays pattern (Fig. 8) reveals stoichiometric existence of the Bi_2S_3 and Bi_2O_3 compound in the film matrix.

A typical XRD pattern for a film prepared under 60 min deposition has been presented in Fig. 9. Different XRD

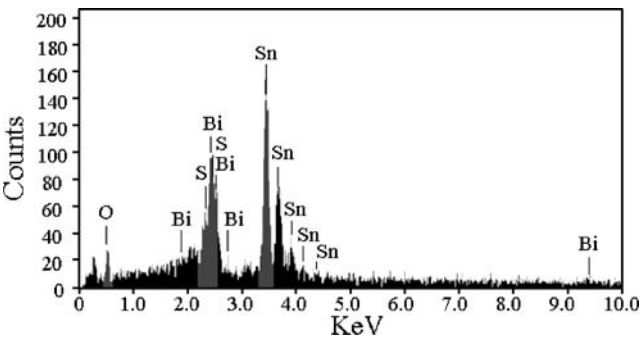

Fig. 8 EDAX analysis of Bi_2S_3 film developed at 60 min deposition from the electrolytic bath containing 0.02 M bismuth nitrate, 0.15 M thiourea, 0.2 M TEA, and 0.5% TX-100, and the current density and temperature maintained at 3 A m^{-2} and 100 °C, respectively

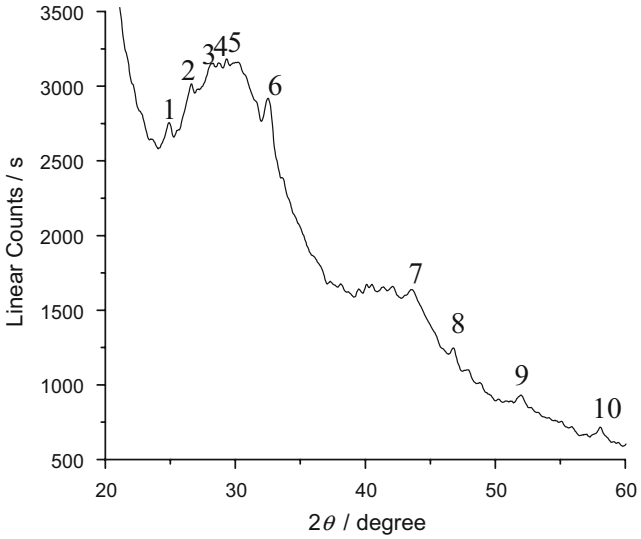

Fig. 9 XRD pattern of Bi_2S_3 thin film for 60 min deposition from the electrolytic bath containing 0.02 M bismuth nitrate, 0.15 M thiourea, 0.2 M TEA, and 0.5% TX-100, and the current density and temperature maintained at 3 A m^{-2} and 100 °C, respectively

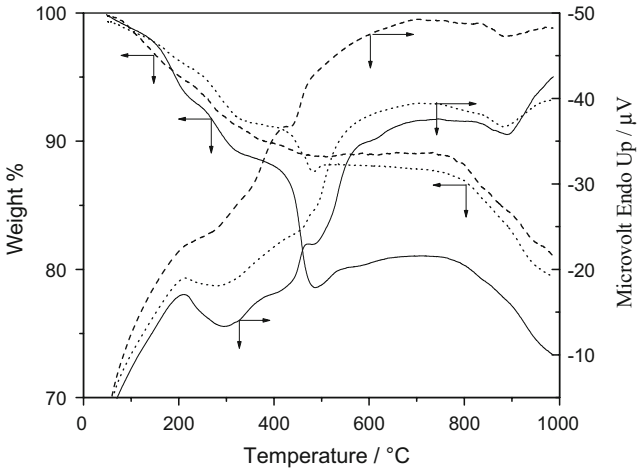

Fig. 10 TG–DTA pattern of Bi_2S_3 film developed at different deposition times: [*dotted lines* 30 min; *solid lines* 45 min; *dashed lines* 60 min] from the electrolytic bath containing 0.02 M bismuth nitrate, 0.15 M thiourea, 0.2 M TEA, and 0.5% TX-100, and the current density and temperature maintained at 3 A m^{-2} and 100 °C, respectively

peaks marked as 1–10 in the figure have been indexed with the help of the JCPDS file [24]. The respective XRD data are summarized in Table 1. The crystallite size falls under the range of 10–15 nm as determined using the Scherrer equation [25]. The lattice parameters indicate the formation of mixed crystals of orthorhombic Bi_2S_3, tetragonal Bi_2O_3, and monoclinic Bi_2O_3.

Figure 10 shows the TG–DTA plots of Bi_2S_3 thin films grown at different deposition times. It was found from TG analysis that the samples prepared under 30 and 45 min restore their stability up to ~440 °C beyond which the respective samples suffer weight loss of 2.97% and 8.17%. This is attributed to the vaporization of excess of elemental S from the matrix preferentially deposited during growth of Bi_2S_3 film [S^{2-}/S (E^0=0.476 V); Bi^{3+}/Bi (E^0=0.308 V)] [26]. The slight increase in percent weight in the TG curve for the material obtained under 45 min deposition is attributed to the formation of some transient/meta-stable compound formation between N_2 and the remaining masses in the system, as reported in the literature [27]. However, with extended deposition for 60 min, the stoichiometric

Table 1 Results of the XRD analysis of the Bi_2S_3 film developed at 60 min deposition time from the electrolytic bath containing 0.02 M bismuth nitrate, 0.15 M thiourea, 0.2 M TEA, and 0.5% TX-100, and the current density and temperature maintained at 3 A m^{-2} and 100 °C, respectively

SL	2θ	I_{rel}	$d=\lambda/2\sin\theta$	Probable identification
1	24.84	86.72	3.59	A(130)(111)
2	26.64	94.86	3.35	B(111)
3	28.23	99.21	3.17	B(012), C(201)
4	28.71	99.00	3.12	A(121)(230), E(300)
5	29.36	100.00	3.05	A(211)(320), D(222)(230)
6	32.52	91.79	2.85	A(040), C(002), D(302)(231)
7	43.52	51.53	2.08	A(250)
8	46.72	39.33	1.95	A(431), C(222)
9	52.01	29.41	1.76	A(620)
10	58.08	22.77	1.59	C(402)

[A = Bi_2S_3 (orthorhombic), B = Bi_2O_3 (monoclinic), C = β-Bi_2O_3 (tetragonal), D = S (monoclinic), E = S (rhombohedral)]

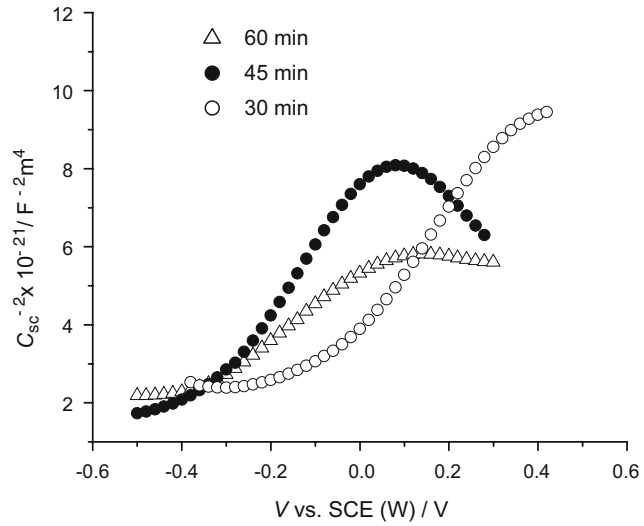

Fig. 11 Mott–Schottky plots for the cell system $Bi_2S_3/S_x^{2-} - S^{2-}/Pt$, using the semiconductor films developed at different deposition times from the electrolytic bath containing 0.02 M bismuth nitrate, 0.15 M thiourea, 0.2 M TEA, and 0.5% TX-100, and the current density and temperature maintained at 3 A m^{-2} and 100 °C, respectively

Table 2 PEC parameters evaluated for the Bi_2S_3 films developed at different temperatures from the electrolytic bath containing 0.02 M bismuth nitrate, 0.1 M thiourea, 0.2 M TEA, and 0.5% TX-100, and the current density and deposition time maintained at 5 A m^{-2} and 45 min, respectively

Bath temperature (°C)	Thickness (μm)	E_g (eV)	$N_d \times 10^{-23}/m^3$	V_{fb} (V)	I_{sc} (A m^{-2}) (*I–V*)	R_{ct} (Ω)	C_{ct} (F)×10^3	%η	%FF
90	0.44	1.39	1.27	−0.371	29.4	232	1.37	0.58	13.81
100	0.65	1.35	1.42	−0.430	25.4	339	1.69	1.01	29.52
110	0.57	1.40	2.75	−0.397	36.3	122	1.56	0.81	17.05

Table 3 PEC parameters evaluated for the Bi_2S_3 films developed at different percentages of TX-100 from the electrolytic bath containing 0.02 M bismuth nitrate, 0.1 M thiourea, and 0.2 M TEA, 3 A m^{-2} current density, and the bath temperature and deposition time maintained at 100 °C and 45 min, respectively

%TX-100	Thickness (μm)	E_g (eV)	$N_d \times 10^{-23}/m^3$	V_{fb} (V)	I_{sc} (A m^{-2}) (*I–V*)	R_{ct} (Ω)	C_{ct} (F)×10^3	%η	%FF
0.0	0.35	1.41	1.85	−0.486	–	–	–	–	–
0.3	0.59	1.40	1.01	−0.458	19.8	458	1.51	0.35	12.59
0.5	0.77	1.40	1.51	−0.296	30.6	333	2.68	0.98	24.61
0.7	0.71	1.38	1.18	−0.705	22.0	150	4.74	1.13	36.81
1.0	0.60	1.41	2.02	−0.346	28.1	143	6.78	1.19	30.39

Table 4 PEC parameters evaluated for the Bi_2S_3 films developed at different concentrations of TEA from the electrolytic bath containing 0.02 M bismuth nitrate, 0.1 M thiourea, and 0.5% TX-100, 3 A m^{-2} current density, and the bath temperature and deposition time maintained at 100 °C and 45 min, respectively

TEA (M)	Thickness (μm)	E_g (eV)	$N_d \times 10^{-23}/m^3$	V_{fb} (V)	I_{sc} (A m^{-2}) (*I–V*)	R_{ct} (Ω)	C_{ct} (F)×0^3	%η	%FF
0.2	0.77	1.40	1.51	−0.296	30.6	333	2.68	0.98	24.61
0.3	0.71	1.43	1.79	−0.648	26.0	517	2.90	0.64	10.67
0.5	0.41	1.46	1.96	−0.873	13.0	496	1.33	0.30	7.14

Table 5 PEC parameters evaluated for the Bi_2S_3 films developed at different deposition times from the electrolytic bath containing 0.02 M bismuth nitrate, 0.15 M thiourea, 0.2 M TEA, and 0.5% TX-100, and the current density and temperature maintained at 3 A m^{-2} and 100 °C, respectively

Deposition time (min)	Thickness (μm)	E_g (eV)	$N_d \times 10^{-23}/m^3$	V_{fb} (V)	I_{sc} (A m^{-2}) (*I–V*)	R_{ct} (Ω)	C_{ct} (F)×10^3	%η	%FF	Decay constant
30	0.43	1.27	0.79	−0.225	28.0	266	1.04	0.80	14.6	0.051
45	0.96	1.35	0.81	−0.468	39.6	167	3.35	0.77	16.0	0.126
60	1.10	1.36	1.48	−0.611	31.5	136	9.30	1.21	26.4	0.116

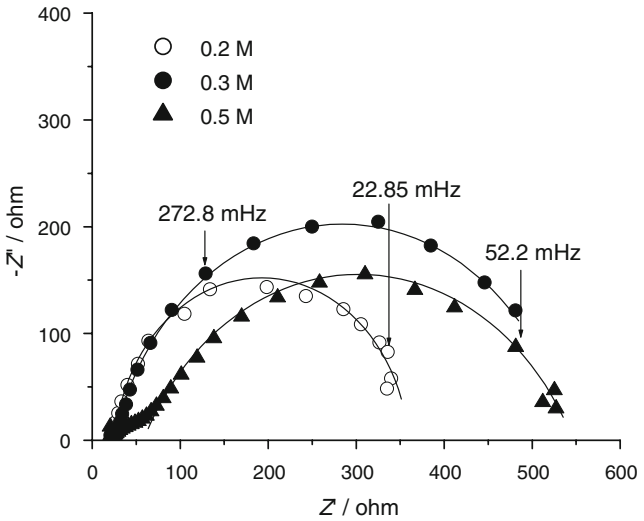

Fig. 12 Nyquist plots of the Bi_2S_3 films developed at different TEA concentrations in electrolytic bath containing 0.02 M bismuth nitrate, 0.1 M thiourea, and 0.5% TX-100, and the current density, deposition time, and temperature maintained at 3 A m^{-2}, 45 min, and 100 °C, respectively

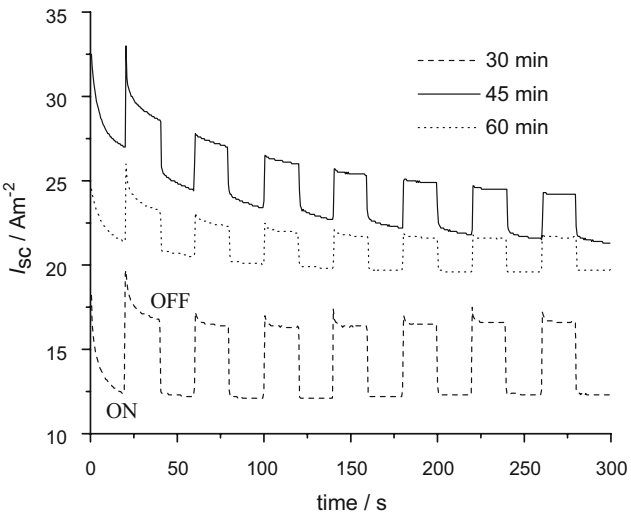

Fig. 14 Short circuit current (I_{sc})–rise and decay curves for the cell system $Bi_2S_3/S_x^{2-} - S^{2-}/Pt$, using the semiconductor films developed at different deposition times from the electrolytic bath containing 0.02 M bismuth nitrate, 0.15 M thiourea, 0.2 M TEA, and 0.5% TX-100, and the current density and temperature maintained at 3 A m^{-2} and 100 °C, respectively

growth of Bi_2S_3 is facilitated and there is no significant weight loss in the TG curve, which indicates the formation of a stable composite film matrix.

The possible reaction pattern of the Bi_2S_3 films subjected to thermal analysis was obtained from the DTA plots. In Fig. 10, the DTA curves do not reveal any significant phase change within the temperature range studied, except a few positive and negative peaks representing exothermic and endothermic reactions, respectively [28, 29]. The endothermic reaction at ~450 °C may be recognized on account of evaporation of the free elemental S on the film surface. The first exothermic peak shows the melting of elemental Bi at 270 °C, whereas the second is attributed to the melting of Bi_2O_3 or Bi_2S_3 at 850 °C.

The Mott–Schottky plots (Fig. 11) for different films are obtained by employing impedance spectroscopic techniques operating on a typical PEC cell configured as $[TCO\ glass/Bi_2S_3/S^{2-} - S_x^{2-}/Pt]$ at a frequency of 1 kHz. The data recorded from capacitance–voltage measurements derive useful information regarding the carrier concentration (N_D), type of conductivity, and the charac-

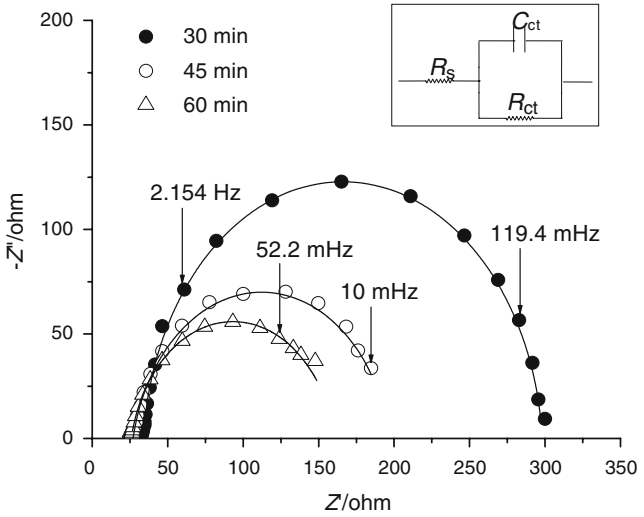

Fig. 13 Nyquist plots of Bi_2S_3 films developed at different deposition times from the electrolytic bath containing 0.02 M bismuth nitrate, 0.15 M thiourea, 0.2 M TEA, and 0.5% TX-100, and the current density and bath temperature maintained at 3 A m^{-2} and 100 °C, respectively

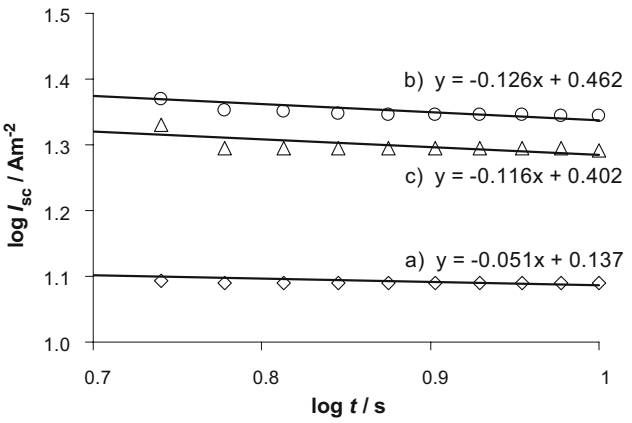

Fig. 15 Variation of log (I_{sc}) vs. log t for the films developed at different deposition times: *a* 30 min, *b* 45 min, and *c* 60 min from the electrolytic bath containing 0.02 M bismuth nitrate, 0.15 M thiourea, 0.2 M TEA, and 0.5% TX-100, and the current density and temperature maintained at 3 A m^{-2} and 100 °C, respectively

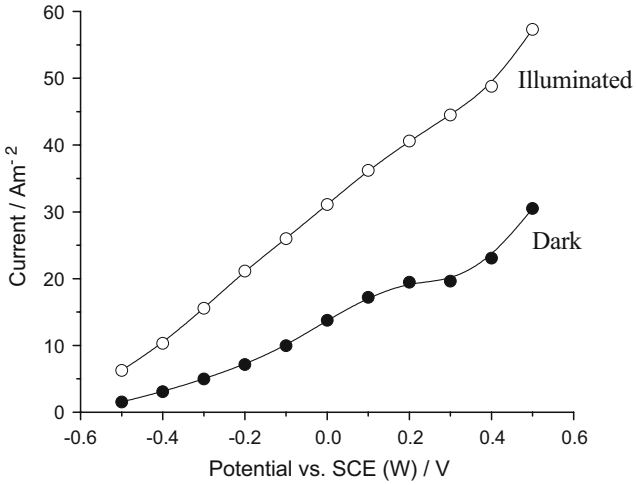

Fig. 16 Potentiostatic polarization for the cell system $Bi_2S_3/S_x^{2-} - S^{2-}/Pt$ in dark and illuminated conditions using the semiconductor films developed at 60 min of deposition from the electrolytic bath containing 0.02 M bismuth nitrate, 0.15 M thiourea, 0.2 M TEA, and 0.5% TX-100, and the current density and temperature maintained at 3 A m^{-2} and 100 °C, respectively

teristics of the SC–electrolyte junction of the PEC cell, by using the Mott–Schottky equation [1, 30]

$$C_{SC}^{-2} = \left(V - V_{fb} - k_B T e^{-1}\right) 2(\varepsilon_0 \varepsilon_S N_D e)^{-1} \quad (2)$$

where V and V_{fb} are respectively the electrode potential and flat band potential, ε_0 and ε_S the permittivities in vacuum and in SC compound, respectively, e is the electronic charge, T the operating temperature (298 K), k_B the Boltzmann's constant, and C_{SC} the space charge

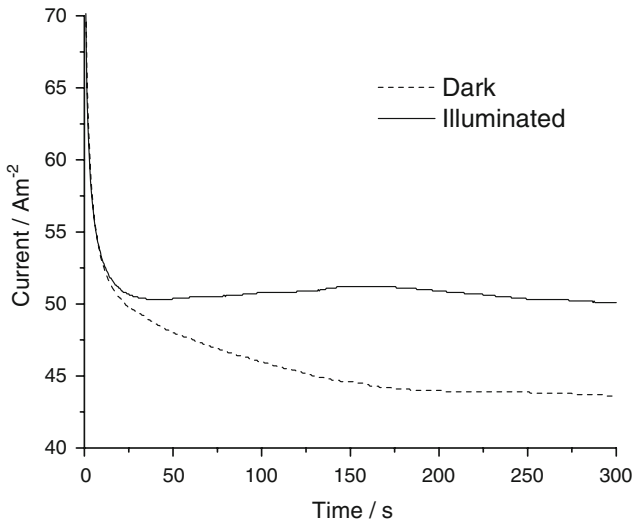

Fig. 17 Chronoamperometric study for the cell system $Bi_2S_3/S_x^{2-} - S^{2-}/Pt$ in dark and illuminated conditions using the semiconductor films developed at 60 min of deposition from the electrolytic bath containing 0.02 M bismuth nitrate, 0.15 M thiourea, 0.2 M TEA, and 0.5% TX-100, and the current density and temperature maintained at 3 A m^{-2} and 100 °C, respectively

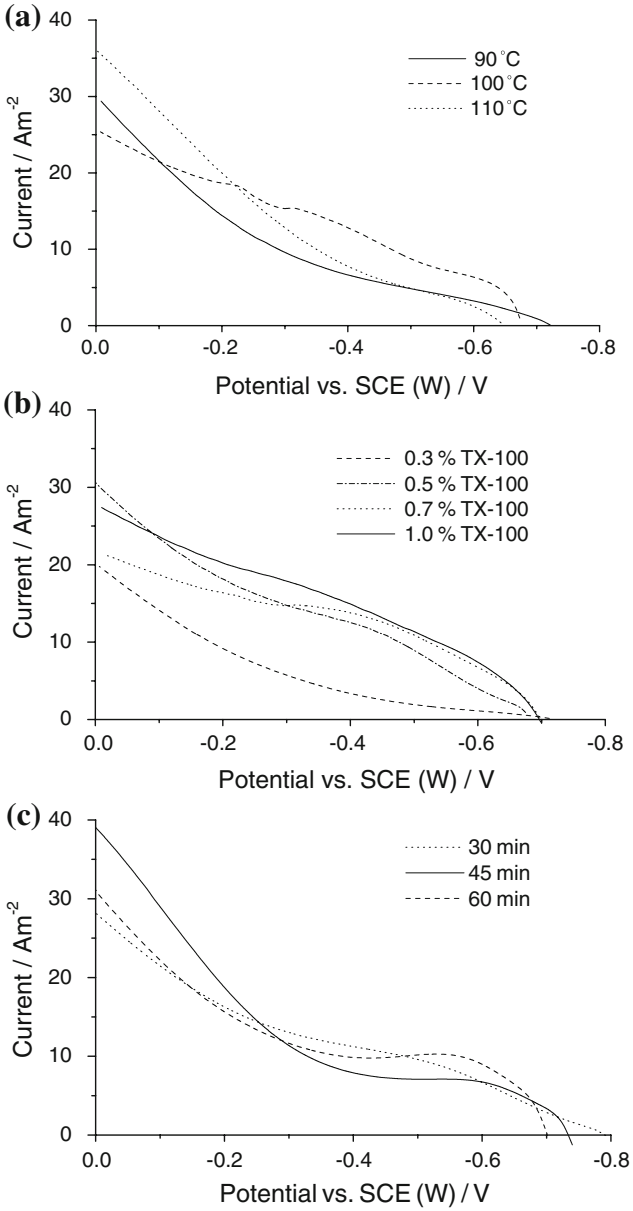

Fig. 18 **a**–**c** Current–potential (*I–V*) curves of the Bi_2S_3 films developed at **a** different bath temperatures, **b** different percentages of TX-100, **c** different deposition times from the electrolytic bath containing 0.02 M bismuth nitrate, 0.15 M thiourea, and 0.2 M TEA, and the current density 3 A m^{-2}

capacitance of the SC film. The evaluated Mott–Schottky parameters are summarized in Tables 2, 3, 4, and 5. The population density of the carrier species is developed with increasing thickness. This partially contributes to build up the desired space charge properties as well as enhances the conductivity of the material. The positive slope of the plot confirmed *n*-type conductivity of the Bi_2S_3 films.

Some of the double layer characteristics developed across the SC/0.5 M Na_2S_x electrolyte interface is displayed in the Nyquist plots (Figs. 12 and 13) derived from the

impedance measurements. The impedance data were further analyzed based upon the simple EC model constituting several circuit components as reported in our earlier studies [1]. In fact, a SC film with low values of R_{ct} and high values of C_{ct} is generally considered suitable as the light absorbing material in PEC cell due to its ability in conduction of charge carrier and storage of charges in the space charge region. The material deposited under time duration of 60 min showed significantly low R_{ct} value (136 Ω) and high capacitance value in contrast with the films obtained under shorter duration of deposition (30 and 45 min) that corresponded to poor performance of PEC character. One interesting feature of the Nyquist plot is the appearance of a tiny semicircle preceding that with the larger diameter as observed in Fig. 12. This is presumably due to the fact that at high concentrations of TEA, the large complex ions get specifically adsorbed on the film surface forming a contact adsorbed layer at the electrode–electrolyte interface. Under the external field, this adsorbed layer is dislodged due to simple charge transfer process, prior to the SC matrix undergoing the typical redox process.

In Fig. 14, instantaneous photoresponse was featured with the rise and decay curves of photocurrent (I_{sc}) during successive exposure of the films to illuminated and dark conditions. Variation of I_{sc} with time found to obey the equation

$$I_{sc}(t) = I_{sc}(0)t^{-b} \quad (3)$$

where $I_{sc}(t)$ and $I_{sc}(0)$ are the short circuit current at time t and 0 s, respectively, and b is the decay constant [1]. The b values for different films were obtained from the linear plots of log I_{sc} vs. log t plot (Fig. 15) and are given in Table 5. The maxima in the b values corresponded to significant absorption property exhibited by the films deposited at 45–60 min.

Potentiostatic polarization curves for the film of 60 min deposition (Fig. 16) clearly indicate consistent enhancement of photocurrent at the respective potentials compared to that in the dark. Long-term stability of the films in the PEC cell system was ascertained through chronoamperometric measurements (Fig. 17) under dark and illuminated conditions. There is a sharp initial current drop followed by an almost invariant progress with the polarization period of 300 s, displaying a much higher current density under exposure to light compared to dark. The power output characteristics of typical PEC cells constituted with the deposited films obtained under variable bath conditions were demonstrated by the current–potential (I–V) curves (Fig. 18a–c) with simultaneous record of the open circuit potentials (V_{oc}) and short circuit currents (I_{sc}). The power conversion efficiency (%η) and fill factor (%FF) were derived from these plots and summarized in Tables 2, 3, 4, and 5. There is a clear trade-off in efficiency with decrease of deposition time. The comparatively thicker films of 45–60 min depositions possess effectively larger solar photon absorbing volume and contribute to the increased short circuit current. Moreover, a considerable thickness imparts a moderately porous texture to the film which further permits the electrolyte to penetrate into the bulk of the crystalline matrix and facilitates the electron-hole separation upon illumination.

Conclusion

Nanostructured films of Bi_2S_3 (n-type) compound semiconductors can easily be grown onto TCO-coated glass through the galvanostatic mode of the electrodeposition technique. The preparative bath condition was judiciously selected by undertaking rigorous optimization process such as altering the parameters like temperature, applied current density, deposition time, and concentration of the complexing agent, surfactant, and the precursor salts. XRD analysis confirms the crystallinity of the film matrix. Compactness and homogeneity of the surface were displayed through the SEM images. The optimal electroplating conditions impart substantial stability to the Bi_2S_3 thin films as revealed in thermal analysis. All the synthesized films with different thickness are of the low band gap regime (1.3–1.9 eV) and are therefore attractive candidates for solar energy conversion. It was found that PEC performance of the film is improved with increasing film thickness. The electrochemical characterizations like potentiostatic polarizations, chronoamperometry, and I–V measurements collectively suggest that the required Bi_2S_3 film can be tailor-made by selecting bath parameters during electrosynthesis. The optimized film achieved significant photoresponsiveness and stability under illumination and thus can be recommended for potential application as photoanode in liquid junction solar cells. This is perhaps an initial approach towards growing high quality Bi_2S_3 films, and the work could be further extended to obtain the global standard method of electroplating of Bi_2S_3 film with the help of statistical designing.

Thus, the simple electrodeposition technique therefore enables optimized growth of Bi_2S_3 film, presenting desired features, by applying the electrolyte bath parameters as furnished below.

Bath temperature	Applied current density	TEA	TX-100	$Bi(NO_3)_3$	Thiourea	Deposition time
100 °C	3 A m^{-2}	0.2 M	0.5%	0.02 M	0.15 M	60 min

Acknowledgment The authors gratefully acknowledge the financial support from University Grant Commission, Defence Research and Development Organizations, New Delhi, Govt. of India.

References

1. Datta J, Bhattacharya C (2007) J Solid State Electrochem 11:215
2. Datta J, Bhattacharya C, Bondhyopadhyay S (2006) Appl Surf Sci 253:2289 doi:10.1016/j.apsusc.2006.04.020
3. Datta J, Bhattacharya C, Bondhyopadhyay S (2006) Appl Surf Sci 252:7493 doi:10.1016/j.apsusc.2005.09.006
4. Datta J, Bhattacharya C (2005) Mater Chem Phys 89:170 doi:10.1016/j.matchemphys.2004.09.002
5. Riley DJ, Waggett JP, Wijayantha KGU (2004) J Mater Chem 14:704 doi:10.1039/b311517h
6. Bessekhouad Y, Mohammedi M, Trari M (2002) Sol Energy Mater Sol Cells 73:339
7. Ricon ME, Campos J, Suarez R (1999) J Phys Chem Solids 60:385 doi:10.1016/S0022-3697(98)00271-6
8. Lu J, Han Q, Yang X, Lu L, Wang X (2007) Mater Lett 61:2883 doi:10.1016/j.matlet.2007.01.071
9. Rincón ME, Hu H, Martínez G, Suárez R, Bañuelos JG (2003) Sol Energy Mater Sol Cells 77:239 doi:10.1016/S0927-0248(02)00345-8
10. Li Q, Shao MW, Wu J et al (2002) Inorg Chem Commun 5:933 doi:10.1016/S1387-7003(02)00604-4
11. Sirimanne PM, Takahashi K, Sonoyama N, Sakata T (2002) Sol Energy Mater Sol Cells 73:175 doi:10.1016/S0927-0248(01)00123-4
12. Lin ZC, Eads CD (1997) Langmuir 13:2647 doi:10.1021/la961004d
13. Peter LM (1979) J Electroanal Chem 98:49 doi:10.1016/S0022-0728(79)80283-1
14. Mane RS, Sankapal BR, Lokhande CD (1999) Mater Chem Phys 60:196 doi:10.1016/S0254-0584(99)00085-1
15. Pejova B, Grozdanov I (2006) Mater Chem Phys 99:39 doi:10.1016/j.matchemphys.2005.10.010
16. Oznuluer T, Demir U (2002) J Electroanal Chem 529:34 doi:10.1016/S0022-0728(02)00921-X
17. Kebbab Z, Benramdane N, Medles M, Bouzidi A, Tabet-Derraz H (2002) Sol Energy Mater Sol Cells 71:449 doi:10.1016/S0927-0248(01)00099-X
18. Li W-H (2008) Mater Lett 62:243 doi:10.1016/j.matlet.2007.05.007
19. Zhu G, Liu P, Zhou J, Bian X, Wang X, Li J, Chen B (2008) Mater Lett available online. doi:10.1016 /j matlet 2007-11-084
20. Lukose J, Pradeep B (1991) Solid State Commun 78:535 doi:10.1016/0038-1098(91)90371-2
21. Hui Y, Dijie H, Zhonghong J, Yong D (1994) J Sol-Gel Sci Technol 3:235 doi:10.1007/BF00486562
22. Memming R (2000) Semiconductor electrochemistry. Willy, Canada
23. Sankapal BR, Lokhande CD (2002) Mater Chem Phys 74:126 doi:10.1016/S0254-0584(01)00414-X
24. JCPDS files: (43-1471, 41-1449, 27-0050, 34-0941, 29-1320)
25. Dewald JF (1959) In: Hannay NB (ed) Semiconductors. Reinfold, New York
26. Lide DR (1998) In: Handbook of chemistry and physics (79th ed) CRC, Boca Raton
27. Dheepa J, Sathyamoorthy, Veluman RS, Subbarayan A, Natarajan K, Sebastian PJ (2004) Sol Energy Mater Sol Cells 81:305 doi:10.1016/j.solmat.2003.11.008
28. Brown ME (2004) In: Introduction to thermal analysis: technique and applications (2nd ed). Kluwer Academic, New York
29. Zielenkiewicz W, Margas E (2004) In: Theory of calorimetry. Kluwer Academic, New York
30. Bard AJ, Faulkner LR (1998) Electrochemical methods. Wiley, New York